Experimental Eye Research 230 (2023) 109441

Contents lists available at ScienceDirect

Experimental Eye Research

journal homepage: www.elsevier.com/locate/yexer

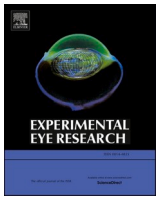

Research article

Quantification of scleral changes during dynamic accommodation

Iulen Cabeza-Gil [a,*], Fabrice Manns [b,c], Begoña Calvo [a,d], Marco Ruggeri [b,c,**]

[a] Aragón Institute of Engineering Research (i3A), University of Zaragoza, Spain
[b] Ophthalmic Biophysics Center, Bascom Palmer Eye Institute, University of Miami Miller School of Medicine, Miami, FL, USA
[c] Department of Biomedical Engineering, University of Miami College of Engineering, Coral Gables, FL, USA
[d] Bioengineering, Biomaterials and Nanomedicine Networking Biomedical Research Centre (CIBER-BBN), Zaragoza, Spain

A B S T R A C T

The mechanics of accommodation is a complex process that involves multiple intraocular ocular structures. Recent studies suggest that there is deformation of the sclera during accommodation that may also play a role in accommodation, influencing ciliary muscle contraction and contributing to the accommodative response. However, the type and magnitude of the deformations measured varies significantly across studies. We present high-resolution synchronous OCT measurements of the anterior sclera contour and thickness and lens thickness acquired in real-time during accommodative responses to 4D step stimuli. The lens thickness was used as an assessment of objective accommodation. No changes in nasal and temporal anterior scleral contour and scleral thickness were found during accommodation within the precision of our measurements. Our results demonstrate that there are no significant scleral deformations during accommodation.

1. Introduction

The mechanics of accommodation is a complex process governed mainly by the lens, zonules and ciliary body (Cabeza-Gil et al., 2021, de Castro et al., 2013; Glasser and Campbell, 1999; Glasser and Kaufman, 1999; Martinez-Enriquez et al., 2017a; Ramasubramanian and Glasser, 2015; Richdale et al., 2013; Wagner et al., 2019). During accommodation the ciliary muscle contracts releasing the resting zonular tension to allow the lens to increase its curvature and thus its refractive power (Glasser and Kaufman, 1999). In addition to these ocular structures, others such as the vitreous, choroid and iris, are also indirectly involved during the accommodation process, which may suggest that they also play a role in accommodation and that their changes with age could also be related to presbyopia to some extent (Croft, Mcdonald, et al., 2013; Croft, Nork, et al., 2013).

More recent studies suggest that there are also changes in the scleral shape that may contribute to the accommodative response (Consejo et al., 2017; Croft et al., 2013; Niyazmand et al., 2020; Woodman-Pieterse et al., 2018). Croft et al. (2013) showed through ultrasound biomicroscopy that the anterior sclera shape in the nasal quadrant changed during accommodation, without any apparent change in the temporal quadrant. Since then, several studies have tried to quantify these changes. Consejo et al. (2017) and Niyazmand et al. (2020) measured the anterior sclera contour during accommodation using profilometry. Even though they used the same instrument, their results differed by two orders of magnitude. Consejo et al. (2017) reported changes in the anterior scleral contour up to 500 μm for a 4D stimulus whilst Niyazmand et al. (2020) reported changes up to 5 μm for a 5D stimulus. Woodman-Pieterse et al. (2018) measured the change in scleral thickness and the total wall thickness (including sclera and conjunctiva) at different locations from the scleral spur in the temporal quadrant using spectral domain optical coherence tomography (SD-OCT) and reported changes of up to 20 μm in the total wall thickness for 6D accommodation stimulus.

Given the large differences across studies in the anterior scleral contour measured during accommodation (Consejo et al., 2017; Niyazmand et al., 2020) and the small amplitude of changes in the scleral thickness [13], the findings remain inconclusive. One of the limitations of the previous studies is that they relied on static measurements at discrete accommodative states, needing an image registration method to correlate the unaccommodated and accommodated state. Static measurements are more sensitive to errors caused by eye movements than dynamic measurements, as it is difficult to image the same scleral part of the subject due to lack of accurate techniques to calibrate the OCT device and the subject in the same position.

The goal of the present study was to quantify the changes in the anterior scleral contour and scleral thickness dynamically during accommodation using high-resolution real-time OCT imaging. The study provide knowledge regarding the role of the sclera during accommodation.

* Corresponding author.
** Corresponding author. Ophthalmic Biophysics Center, Bascom Palmer Eye Institute, University of Miami Miller School of Medicine, Miami, FL, USA.
E-mail addresses: iulen@unizar.es (I. Cabeza-Gil), MRuggeri@med.miami.edu (M. Ruggeri).

https://doi.org/10.1016/j.exer.2023.109441
Received 2 September 2022; Received in revised form 11 January 2023; Accepted 16 March 2023
Available online 22 March 2023

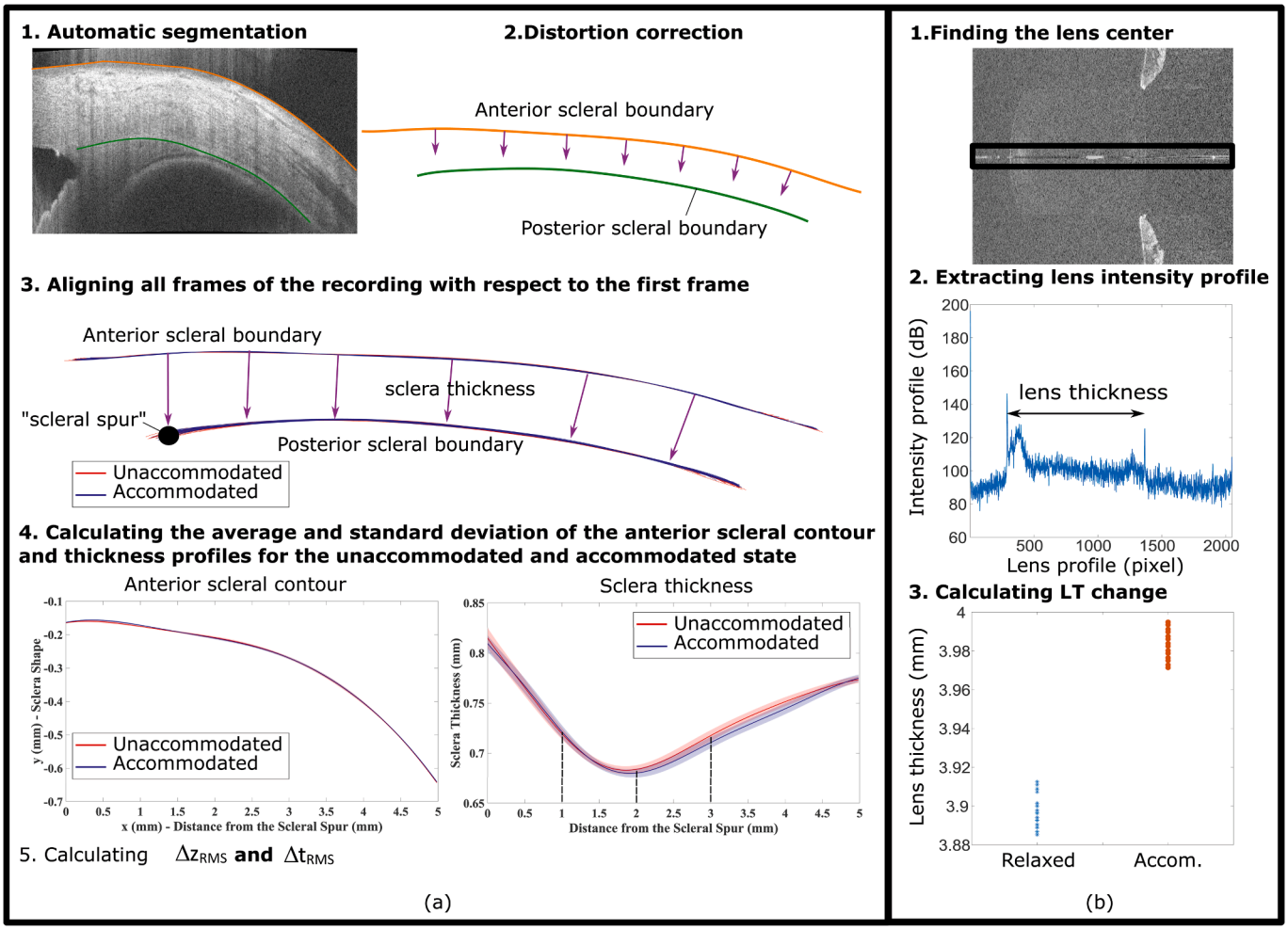

Fig. 1. Methodology to calculate the change in the anterior sclera contour and thickness (a) and lens thickness (b) between the unaccommodated and accommodated state. (a) Each frame is segmented by a fully convolutional network (Cabeza-Gil et al., 2022) and corrected for distortion. In the sclera shape and thickness profiles, the shaded area is the standard deviation whilst the thick line is the average of the measurements.

2. Methods

2.1. Study design

This prospective study was carried out at the Bascom Palmer Eye Institute, University of Miami Miller School of Medicine with approval from the Institutional Review Board at the University of Miami while following the tenets of the Declaration of Helsinki. Written informed consent was obtained for all participants. The experiments were performed on the temporal and nasal quadrants of the left eye of 10 young healthy subjects (age: 26.1 ± 3.66 y/o, range: 20 to 31 y/o) with average refractive error of −0.53 ± 1.35 D (range: −3.25 to 1.75 D).

2.2. Imaging protocol

The imaging unit consists of two separate SD-OCT systems operating at central wavelengths of 1325 nm and 840 nm for acquiring transscleral ciliary muscle and anterior segment images, respectively, at a frame rate of 13 Hz. Anterior segment images were used to confirm that all subjects accommodated during the experiments by quantifying the changes in lens thickness (LT) during accommodation. The OCT systems were combined and synchronized with a dual-channel visual fixation target designed to produce step stimuli of accommodation during OCT image acquisition. Details about the individual OCT systems and accommodative fixation target were previously reported (Ruggeri et al., 2012, 2014). Briefly, imaging of the full anterior segment at 840 nm was achieved with a custom-made SD-OCT unit that features extended axial range (Ruggeri et al., 2012), whereas a commercially available research SD-OCT system (TELESTO, Thorlabs Inc., NJ) operating at 1325 nm was used for ciliary muscle imaging.

Subjects were seated in front of the instrument with their head stabilized in a chin rest and contour head frame. The visual fixation target was aligned to avoid convergence and ensure that the eye remains co-aligned with the OCT systems during the step accommodative response. The fixation target was programmed to apply a 4D step stimulus. The step stimulus is produced by rapidly switching off/on a fixation target located in the far/near channel of the accommodative fixation target, respectively [15,16]. Anterior segment and transscleral OCT images were acquired in real-time during the accommodative response. Each recording lasted 6.17 s and the accommodation step stimulus was triggered 1.54 s after the start of an acquisition. As a control, a recording with both the far and near targets set at 0D (no accommodation stimulus) was performed for five of the ten subjects. A recording was performed in the nasal and temporal quadrant of each subject. Each recording consisted of a sequence of 160 OCT images of the transscleral ciliary muscle [512 × 897 pixels] and the anterior segment [400 × 2048 pixels]. The pixel density along the height and width of the transscleral images was 512 pixels/2.5 mm and 897 pixels/10 mm, respectively, see Fig. 1a.

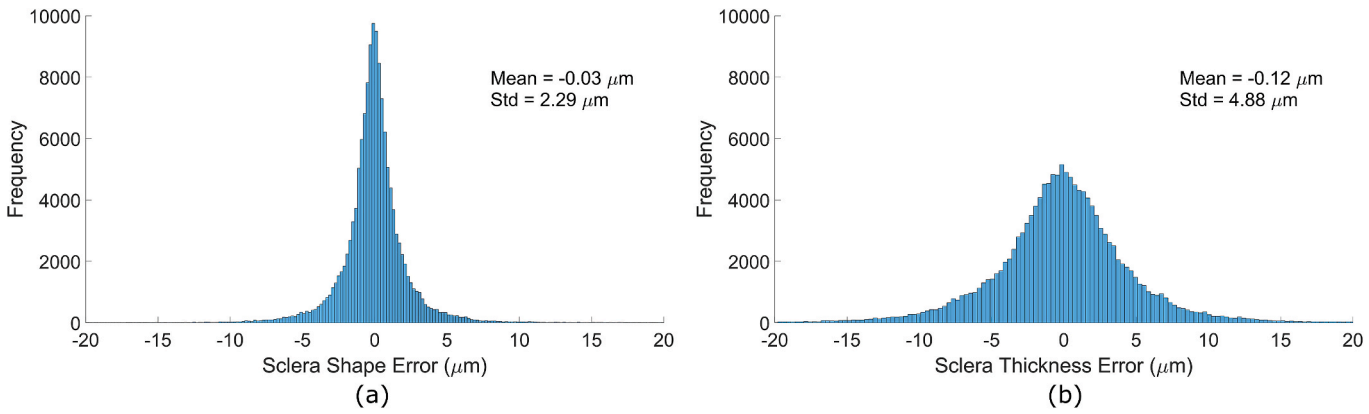

Fig. 2. Histogram to compare the anterior scleral contour (a) and scleral thickness (b) measurements. The confidence interval 95% (CI) for the scleral contour and the sclera thickness measurements were [-4.62, 4.56 μm] and [-9.72, 9.48 μm], respectively. There were 500 points for every scleral contour and scleral thickness profile and at least 10 profiles in each accommodative state (unaccommodated or accommodated) for each subject, resulting in two histograms composed of 139,000 points.

2.3. Image post-processing and data analysis

The first 40 (unaccommodated state) and last 40 (accommodated state) frames of each recording were analyzed. The transscleral OCT images, both in nasal and temporal quadrant, were segmented with a custom-developed automatic tool described elsewhere (Cabeza-Gil et al., 2022) to quantify the sclera deformation between the unaccommodated and accommodated state. Due to variations in image quality, and shadowing by blood vessels, the scleral boundaries could not be accurately segmented in all images. For quality control, a single examiner visually assessed the accuracy of the segmentations. Images where the boundary was not accurately segmented were discarded. A minimum of 10 images for each accommodative state were used. A distortion correction algorithm was applied to the selected images to correct for distortions due to refraction of the OCT beam at the air-sclera boundary (Monterano Mesquita et al., 2021; Ruggeri et al., 2014).

Fig. 1 summarizes the methodology used in this study. The anterior and posterior contour of the sclera were registered with reference to the first frame. Then, the average anterior and posterior scleral contour for the selected images were calculated. The anterior scleral contour and the scleral thickness in the unaccommodated and accommodated state were calculated from these average contours. The anterior scleral boundary was defined as the outermost boundary (including the conjunctiva).

The change in the anterior scleral contour was calculated as the root mean square difference (Δz_{RMS}) between the average scleral contour in the unaccommodated and accommodated state. The scleral thickness was calculated at each pixel by measuring the distance from the anterior to the posterior scleral boundary along a line that is perpendicular to the anterior boundary (Fig. 1, magenta arrow). The change in the scleral thickness was quantified as the root mean square difference (Δt_{RMS}) between the average unaccommodated and accommodated thickness profile. Both the anterior scleral contour and the scleral thickness profile were composed of 500 data points. Note that the change in the anterior scleral contour only accounts for the vertical distance whilst the scleral thickness is measured diagonally (considering vertical and horizontal pixels).

To quantify local changes that may be undetected when the root mean square difference is used as a metric, the scleral thickness was also measured at 1.0, 2.0 and 3.0 mm from the scleral spur similarly to previous reports (Woodman-Pieterse et al., 2018).

A custom automated segmentation algorithm was applied to each of the 80 OCT images of the anterior segment to detect the boundaries of the lens and calculate the central thickness (Ruggeri et al., 2016). The measured optical thickness was converted into geometrical lens thickness assuming an average group refractive index of 1.40 for the lens.

The reliability of the measurements was estimated through repeatability tests. These tests calculate the variability of the measurements, including instrument variability and variability of the segmentation tool (Cabeza-Gil et al., 2022). To do so, for each individual profile recorded during the imaging sequence and included in the analysis, the difference between the profile and the average profile was calculated for each of the 500 data points. The analysis was conducted for anterior and

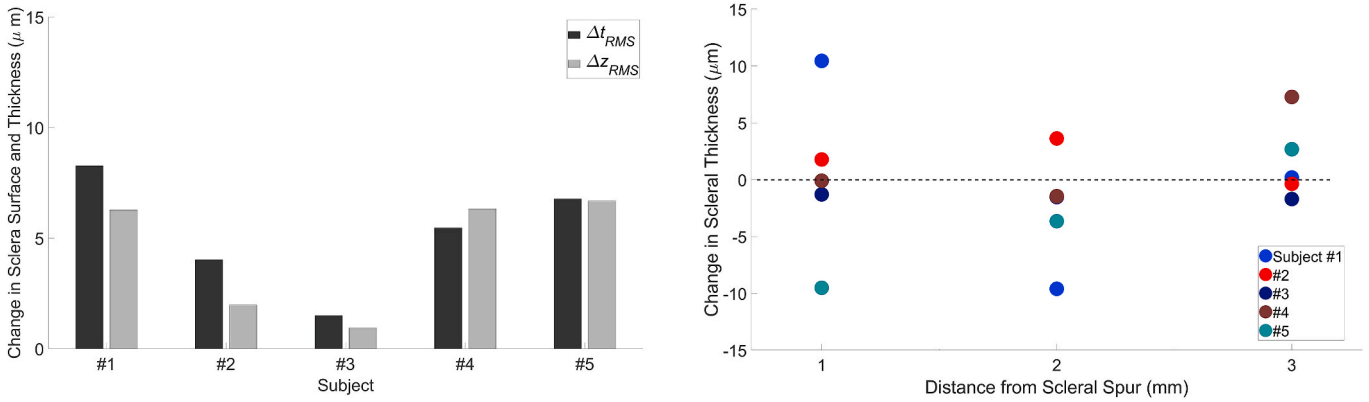

Fig. 3. (a) Change registered in the control tests for the sclera shape (Dz_{RMS}) and sclera thickness (Dt_{RMS}) between the first and last 40 frames of the recording. Measurements were performed in the temporal side for subjects #1, #2 and #3 and in the nasal side for subjects #4 and #5. (b) Change in scleral thickness registered at 1.0, 2.0 and 3.0 mm from the scleral spur for the five control tests.

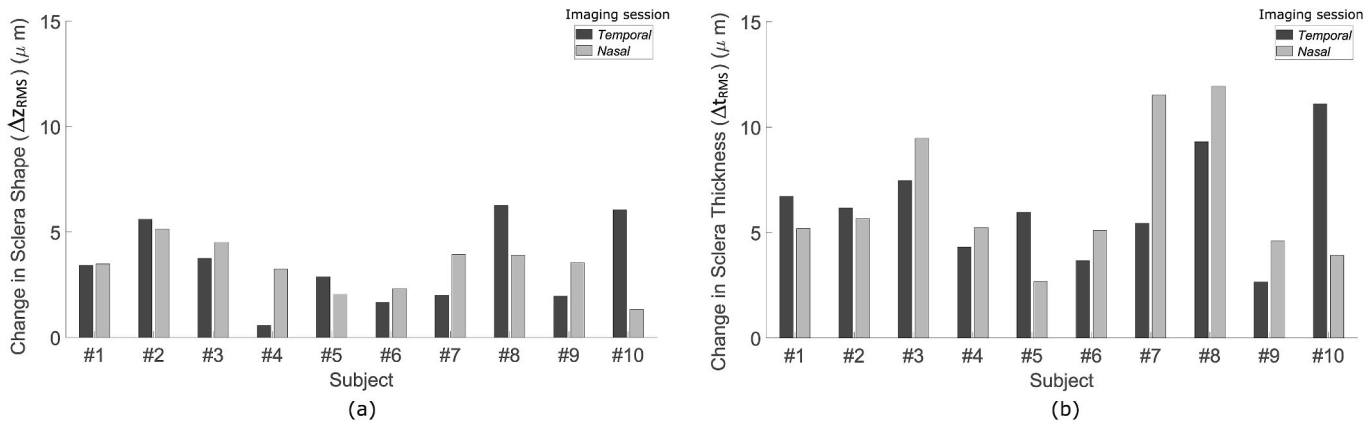

Fig. 4. Change in the anterior sclera shape (a) and thickness (b) for the temporal and nasal side. The changes are defined at the root mean square difference between the relaxed and accommodated state over the 500 points that compose every profile.

posterior scleral contours and scleral thickness. Measurements from all subjects in both the unaccommodated and accommodated states were combined for this analysis. We estimated the precision of the methodology as the standard deviation (SD) of all the samples (Fig. 2).

The precision of the methodology, which account for instrument variability plus potential eye movements, was calculated through control tests. The level of precision of each measurement was calculated as the variability range obtained in the control tests.

2.4. Statistical analysis

A two-sample *t*-test with a significance level of 0.05 was used among the control group and the experimental tests to determine if there was a statistically significant difference between the relaxed and accommodated state for the anterior scleral contour and scleral thickness. All data processing was performed with MATLAB R2022a.

3. Results

3.1. Repeatability of the measurements

The SD of the anterior sclera contour and sclera thickness measurements were 2.29 μm and 4.88 μm, respectively (Fig. 2), which correspond to a repeatability (defined as one standard deviation) of less than one image pixel (4.88 μm × 11.14 μm; horizontal × vertical) in the anterior scleral contour and the scleral thickness measurements. The histogram (Fig. 2) shows that the error is normally distributed with a bias near zero, suggesting that changes recorded during the repeatability study are likely due to the uncertainty of the measurements and unrelated to actual changes in the sclera.

3.2. Control experiments

Fig. 3a shows the change in the anterior scleral contour and thickness for the control experiments where subjects responded to a 0D accommodation stimulus. Although the amplitude of the accommodation stimulus was 0 D, the visual target was switched between the far and near channels to assess the variability of the methodology (i.e. eye movements induced by the stimulus change and instrument variability). There was no significant change in lens thickness (range = −0.03 to 0.04 mm; mean ± std = 0.00 ± 0.02 mm) for any of the subjects during the control experiment, confirming that the subjects did not accommodate.

The change in scleral contour (Δz_{RMS}) and thickness (Δt_{RMS}) ranged from 0.9 to 6.8 μm (mean ± std = 4.4 ± 2.7 μm) and from 1.5 to 8.3 μm (mean ± std = 5.2 ± 2.6 μm), respectively. Fig. 3b shows the change of the scleral thickness at 1.0, 2.0 and 3.0 mm from the scleral spur for the five control tests. The scleral thickness difference (Δt) at 1.0, 2.0 and 3.0 mm from the scleral spur ranged from −9.5 to 10.4 μm (mean ± std = 0.2 ± 7.1 μm), −9.6 to 3.6 μm (mean ± std = −2.5 ± 4.7 μm), and from −1.7 to 7.3 μm (mean ± std = 1.6 ± 3.5 μm), respectively. Negative values indicate a thinning whilst positive values indicate a thickening of the sclera. Overall, the variability of the control experiment is slightly larger than the variability obtained from the repeatability study. This finding suggests that residual changes in gaze when the visual fixation target is switched from the far to the near channel may contribute to

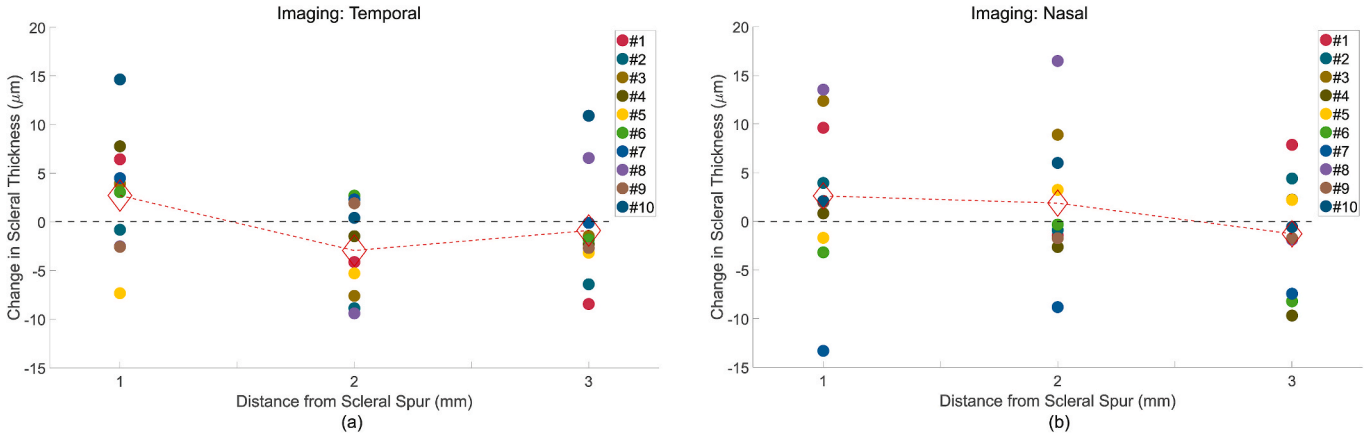

Fig. 5. Changes in the scleral thickness at 1.0, 2.0 and 3.0 mm from the scleral spur in the temporal (a) and nasal (b) quadrant. The red diamonds represent the mean for each position. (For interpretation of the references to colour in this figure legend, the reader is referred to the Web version of this article.)

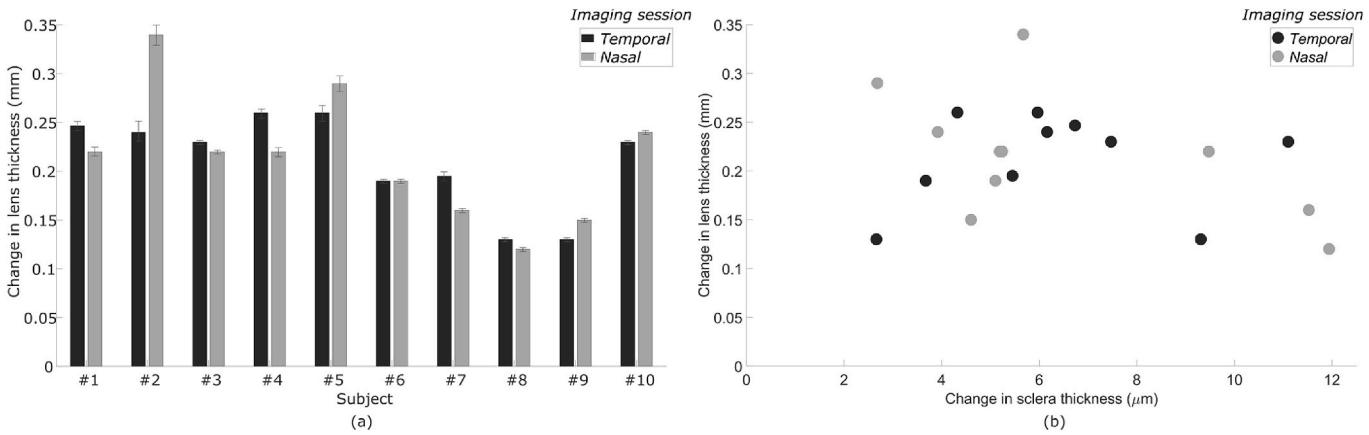

Fig. 6. (a) Change in lens thickness in response to a 4D stimulus for the 10 subjects. The dark and light bars are the measurements acquired when the sclera was imaged in the temporal/nasal quadrant, respectively. (b) Change in the scleral thickness vs change in the LT. Both temporal and nasal measurements are plotted in the graph. A linear regression analysis between the change in lens scleral thickness and lens thickness found no statistically significant relation ($p = 0.18$).

increasing the variability of the methodology.

3.3. Scleral changes during accommodation

Fig. 4 presents the changes in scleral shape (Δz_{RMS}) and thickness Δt_{RMS} in the temporal and nasal quadrant for the 10 subjects during accommodation. Δz_{RMS} ranged from 0.6 to 6.3 μm (mean ± std = 3.4 ± 2.0) and from 1.3 to 5.1 μm (mean ± std = 3.3 ± 1.2) in the temporal and nasal quadrant, respectively. Δt_{RMS} ranged from 2.6 to 11.1 μm (mean ± std = 6.3 ± 2.6) and from 2.7 to 11.9 μm (mean ± std = 6.5 ± 3.2) in the temporal and nasal quadrant, respectively. These changes are comparable to those obtained in the control experiments. In four measurements out of 20 (subjects #7 nasal, #8 nasal and temporal and #10 temporal) the measured thickness change was higher than in the control experiments (difference up to 3.6 μm).

However, no statistically significant difference was found between these tests and the control group for the scleral contour ($p = 0.40$) and for the scleral thickness ($p = 0.38$). We found also no statistically significant difference between the temporal and nasal side neither for the scleral contour ($p = 0.77$) nor thickness ($p = 0.85$).

Fig. 5 shows the changes in the scleral thickness at 1.0, 2.0 and 3.0 mm from the scleral spur for the temporal and nasal quadrant. The thickness change is comparable to the variability measured in the control experiments (0D stimulus), suggesting that if there is a local deformation in the sclera during accommodation, it is below the level of variability of the methodology (~20 μm, calculated from the variability range obtained in the control tests [−9.5,10.4 μm]). No statistically significant difference was found between the control group and these tests ($p = 0.72$), between the temporal and nasal quadrants ($p = 0.81$), and between any scleral thickness at different distances from the scleral spur.

3.4. Lens change during accommodation

All subjects accommodated in response to the accommodation stimuli (Fig. 6a). The change in lens thickness for a 4D accommodation stimulus ranged from 0.13 to 0.31 mm (mean ± std = 0.21 ± 0.05 mm). Given that the lens thickness change across subjects ranges approximately from 30 to 60 μm per D of accommodation (Khan et al., 2018; Martinez-Enriquez et al., 2017b; Richdale et al., 2008; Xiang et al., 2021), these changes suggest an objective accommodation between 2D and 4D. There was no correlation between the change in scleral thickness (Δt_{RMS}) and the change in LT (Fig. 6b) for the temporal ($p = 0.75$) and nasal ($p = 0.09$) quadrant.

4. Discussion

This study aimed at evaluating the changes in scleral shape during accommodation. For this purpose, we measured the sclera deformation (anterior scleral contour and the scleral thickness) in response to a 4D accommodation step stimulus. No changes in shape of the sclera due to accommodation were observed at the level of precision of the current methodology. (~7, 10 and 20 μm for the scleral contour, thickness and local thickness, respectively). The differences in scleral shape with accommodation were the same as in the control group which responded to a 0D stimulus.

Croft et al. (2013) pharmacologically induced accommodation in 12 human subjects (ages 19–65 years) and observed that the sclera deformed in the nasal quadrant during accommodation, with the formation of a notch for young subjects and inward bowing for old ones. They did not observe those changes for the temporal quadrant. We did not observe such changes, as shown in Videos #1 and #2 recorded in the nasal quadrant on two different subjects with two different incidence angles. In addition, our results show non-significant changes in scleral contour of more than an order of magnitude smaller than those found using ocular profilometry by Consejo et al. (2017), who reported an average change in the anterior nasal scleral contour of 390 ± 330 μm for a 4D accommodation stimulus. The incorporation of image registration to control for accommodative convergent and torsional eye movements most probably accounts for the observed differences between our study and the Croft et al. (2013) and the Consejo et al. (2017) studies (Schachar, 2021).

Supplementary video related to this article can be found at https://doi.org/10.1016/j.exer.2023.109441

Our results are closer to those of Woodman-Pieterse et al. (2018) who quantified the change in scleral thickness for myopes ($n = 18$) and emmetropes ($n = 15$) at 1.0, 2.0 and 3.0 mm from the scleral spur for 3D and 6D accommodation stimuli. They used a commercial OCT system and segmented with a semi-automatic tool provided by the OCT manufacturer. They found small changes in thickness (8 μm for a 6 D stimulus), with a difference between myopes and emmetropes at 3D, but not at 6D. They also found a significant variability with measurement location. The large differences across locations and inconsistencies between the responses at 3D and 6D could reflect uncertainties due to the measurement variability (approximately 10 μm according to Read et al. (2016)), which is on the order of the changes that were measured.

The prior studies relied on measurements obtained from single images acquired in the unaccommodated and accommodate states. Our ability to measure scleral shape in real-time on multiple frames (160) and segment these large sets of images with an automatic tool (Cabeza-Gil et al., 2022) during dynamic accommodative responses helps

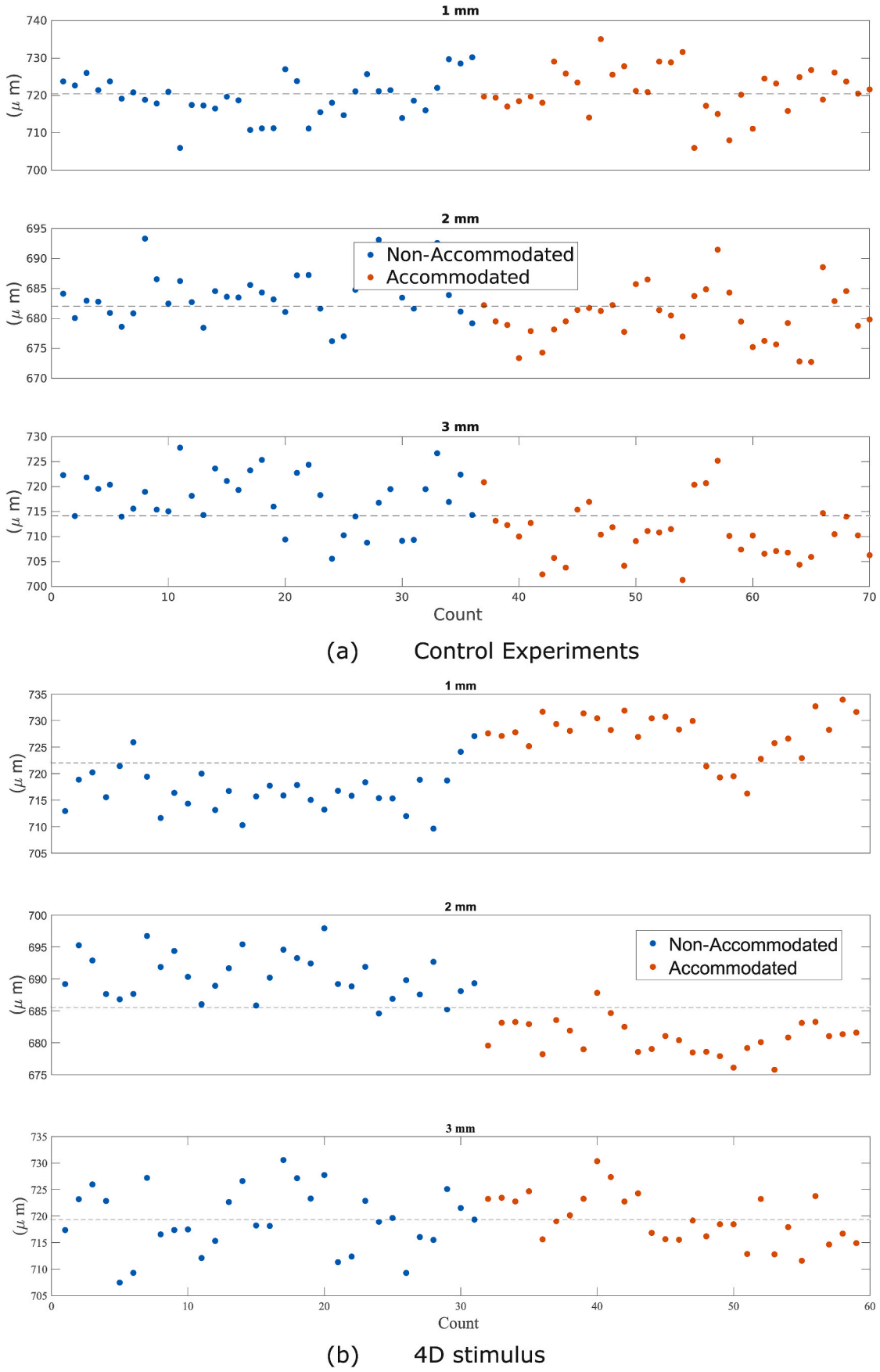

Fig. 7. Sclera thickness at 1.0, 2.0 and 3.0 mm from the scleral spur for a 4D and 0D (control test) accommodation stimuli for the same subject #1.70 and 59 frames were registered for (a) and (b), respectively). The horizontal dashed line is the average value.

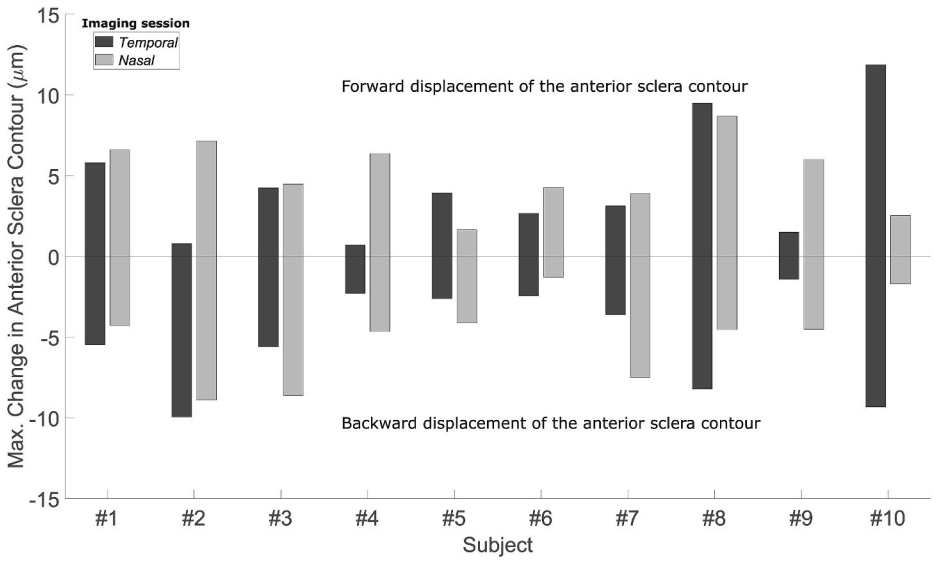

Fig. 8. Max. difference between the unaccommodated and accommodated anterior sclera contour. Negative values indicate a thinning whilst positive values indicate a thickening.

quantify scleral changes with higher confidence. As an example, we plotted the sclera thickness obtained from each individual frame at 1.0, 2.0. and 3.0 mm from the scleral spur for subject #1 (Fig. 7a). The figure illustrates the large frame-by-frame variability of the local measurement, mainly caused by uncertainty in the segmentation and eye movements. The variability is consistent with the histogram of Fig. 2 (approximately±10 μm, corresponding to±2 pixels). It highlights the need to compare scleral profiles when quantifying scleral changes rather than local points, which are subject to greater variability. Moreover, it shows the advantage of averaging many measurements performed on multiple frames with image registration (see Fig. 8).

Niyazmand et al. (2020) did not find any difference between myopes (n = 18) and emmetropes (n = 18) in anterior scleral changes. They reported a statistically significant change of 5 μm in the anterior sclera contour for a 5D stimulus using profilometry. To compare our results to their findings [12], we calculated the maximum difference between the averaged relaxed and accommodated anterior scleral profiles for all subjects (Fig. 7). The maximum change in sclera shape was 11.3 μm (subject #10). Across subjects, the measurements ranged from negative to positive values.

One of the main limitations that is common across all the studies on scleral changes with accommodation, including ours, is that residual ocular convergence during accommodation might affect the measurements of scleral shape. However, the advantage of our method over prior ones is that it allows to record the dynamic sequences (video #1 and #2) of the sclera during accommodation and perform registration to minimize the effect of convergence or even to retake the measurements if large eye motion artifacts are visually detected in the video sequences (Monterano Mesquita et al., 2021).

In summary, our study found that there are no significant changes in scleral contour and thickness during accommodation within the measurement precision provided by our methodology.

Declaration of competing interest

The authors declare no conflicts of interest.

Data availability

Data will be made available on request.

Acknowledgments

I. Cabeza-Gil gratefully acknowledges research support from *the Margarita Salas postdoctoral fellowship funded by Ministerio de Universidades (Spain) and UnionEuropea*-NextGenerationEU. The study was supported by National Eye Institute Grants R01EY014225, P30EY14801 (Center Core Grant); the Florida Lions Eye Bank and Beauty of Sight Foundation; the Henri and Flore Lesieur Foundation (JMP); Drs. Harry W. Flynn Jr MD, Raksha Urs, PhD and Aaron Furtado; Karl R. Olsen, MD and Martha E. Hildebrandt, PhD; an PID2020-113822RB-C21/funded by MCIN/AEI/10.13039/501100011033.

References

Cabeza-Gil, I., Grasa, J., Calvo, B., 2021. A validated finite element model to reproduce Helmholtz's theory of accommodation: a powerful tool to investigate presbyopia. Ophthalmic Physiol. Opt. https://doi.org/10.1111/opo.12876.

Cabeza-Gil, I., Ruggeri, M., Chang, Y.-C., Calvo, B., Manns, F., 2022. Automated segmentation of the ciliary muscle in OCT images using fully convolutional networks. Biomed. Opt Express 13 (5). https://doi.org/10.1364/boe.455661.

Consejo, A., Radhakrishnan, H., Iskander, D.R., 2017. Scleral changes with accommodation. Ophthalmic Physiol. Opt. 37 (3) https://doi.org/10.1111/opo.12377.

Croft, M.A., Mcdonald, J.P., Katz, A., Lin, T.L., Lütjen-Drecoll, E., Kaufman, P.L., 2013a. Extralenticular and lenticular aspects of accommodation and presbyopia in human versus monkey eyes. Invest. Ophthalmol. Vis. Sci. 54 (7) https://doi.org/10.1167/iovs.12-10846.

Croft, M.A., Nork, M.T., Mcdonald, J.P., Katz, A., Lütjen-Drecoll, E., Kaufman, P.L., 2013b. Accommodative movements of the vitreous membrane, choroid, and sclera in young and presbyopic human and nonhuman primate eyes. Invest. Ophthalmol. Vis. Sci. 54 (7) https://doi.org/10.1167/iovs.12-10847.

de Castro, A., Birkenfeld, J., Maceo, B., Manns, F., Arrieta, E., Parel, J.M., Marcos, S., 2013. Influence of shape and gradient refractive index in the accommodative changes of spherical aberration in nonhuman primate crystalline lenses. Invest. Ophthalmol. Vis. Sci. 54 (9) https://doi.org/10.1167/iovs.13-11996.

Glasser, A., Campbell, M.C.W., 1999. Biometric, optical and physical changes in the isolated human crystalline lens with age in relation to presbyopia. Vis. Res. 39 (11), 1991–2015. https://doi.org/10.1016/s0042-6989(98)00283-1.

Glasser, A., Kaufman, P.L., 1999. The mechanism of accommodation in primates. Ophthalmology 106 (5). https://doi.org/10.1016/S0161-6420(99)00502-3.

Khan, A., Pope, J.M., Verkicharla, P.K., Suheimat, M., Atchison, D.A., 2018. Change in human lens dimensions, lens refractive index distribution and ciliary body ring diameter with accommodation. Biomed. Opt Express 9 (3). https://doi.org/10.1364/boe.9.001272.

Martinez-Enriquez, E., Pérez-Merino, P., Velasco-Ocana, M., Marcos, S., 2017a. OCT-based full crystalline lens shape change during accommodation in vivo. Biomed. Opt Express 8 (2). https://doi.org/10.1364/boe.8.000918.

Martinez-Enriquez, E., Pérez-Merino, P., Velasco-Ocana, M., Marcos, S., 2017b. OCT-based full crystalline lens shape change during accommodation in vivo. Biomed. Opt Express 8 (2). https://doi.org/10.1364/boe.8.000918.

Monterano Mesquita, G., Patel, D., Chang, Y.-C., Cabot, F., Ruggeri, M., Yoo, S.H., Ho, A., Parel, J.-M.A., Manns, F., 2021. In vivo measurement of the attenuation coefficient of the sclera and ciliary muscle. Biomed. Opt Express 12 (8). https://doi.org/10.1364/boe.427286.

Niyazmand, H., Read, S.A., Atchison, D.A., Collins, M.J., 2020. Effects of accommodation and simulated convergence on anterior scleral shape. Ophthalmic Physiol. Opt. 40 (4) https://doi.org/10.1111/opo.12697.

Ramasubramanian, V., Glasser, A., 2015. Objective measurement of accommodative biometric changes using ultrasound biomicroscopy. J. Cataract Refract. Surg. 41 (3) https://doi.org/10.1016/j.jcrs.2014.08.033.

Read, S., Alonso-Caneiro, D., Vincent, S., et al., 2016. Anterior eye tissue morphology: Scleral and conjunctival thickness in children and young adults. Sci. Rep. 6, 33796. https://doi.org/10.1038/srep33796.

Richdale, K., Bullimore, M.A., Zadnik, K., 2008. Lens thickness with age and accommodation by optical coherence tomography. Ophthalmic Physiol. Opt. 28 (5) https://doi.org/10.1111/j.1475-1313.2008.00594.x.

Richdale, K., Sinnott, L.T., Bullimore, M.A., Wassenaar, P.A., Schmalbrock, P., Kao, C.Y., Patz, S., Mutti, D.O., Glasser, A., Zadnik, K., 2013. Quantification of age-related and per diopter accommodative changes of the lens and ciliary muscle in the emmetropic human eye. Invest. Ophthalmol. Vis. Sci. 54 (2) https://doi.org/10.1167/iovs.12-10619.

Ruggeri, M., de Freitas, C., Williams, S., Hernandez, V.M., Cabot, F., Yesilirmak, N., Alawa, K., Chang, Y.-C., Yoo, S.H., Gregori, G., Parel, J.-M., Manns, F., 2016. Quantification of the ciliary muscle and crystalline lens interaction during accommodation with synchronous OCT imaging. Biomed. Opt Express 7 (4). https://doi.org/10.1364/boe.7.001351.

Ruggeri, M., Hernandez, V., de Freitas, C., Manns, F., Parel, J.-M., 2014. Biometry of the ciliary muscle during dynamic accommodation assessed with OCT. Ophthalmic Technol. XXIV, 8930. https://doi.org/10.1117/12.2044309.

Ruggeri, M., Uhlhorn, S.R., de Freitas, C., Ho, A., Manns, F., Parel, J.-M., 2012. Imaging and full-length biometry of the eye during accommodation using spectral domain OCT with an optical switch. Biomed. Opt Express 3 (7). https://doi.org/10.1364/boe.3.001506.

Schachar, R.A., 2021. Image registration is required for experiments of accommodation. Invest. Ophthalmol. Vis. Sci. 62 (Issue 2) https://doi.org/10.1167/IOVS.62.2.17.

Wagner, S., Zrenner, E., Strasser, T., 2019. Emmetropes and myopes differ little in their accommodation dynamics but strongly in their ciliary muscle morphology. Vis. Res. 163 https://doi.org/10.1016/j.visres.2019.08.002.

Woodman-Pieterse, E.C., Read, S.A., Collins, M.J., Alonso-Caneiro, D., 2018. Anterior scleral thickness changes with accommodation in myopes and emmetropes. Exp. Eye Res. 177 https://doi.org/10.1016/j.exer.2018.07.023.

Xiang, Y., Fu, T., Xu, Q., Chen, W., Chen, Z., Guo, J., Deng, C., Manyande, A., Wang, P., Zhang, H., Tian, X., Wang, J., 2021. Quantitative analysis of internal components of the human crystalline lens during accommodation in adults. Sci. Rep. 11 (1) https://doi.org/10.1038/s41598-021-86007-6.